

11/5/90  
E5631

NASA Technical Memorandum 103266

# Uses of Auger and X-ray Photoelectron Spectroscopy in the Study of Adhesion and Friction

Kazuhisa Miyoshi  
*Lewis Research Center  
Cleveland, Ohio*

Prepared for the  
First International Symposium on Industrial Tribology  
sponsored by the National Science Foundation Industry/University Cooperative  
Research Center for Engineering Tribology at Northwestern University  
Chicago, Illinois, August 29-31, 1990

**NASA**

# USES OF AUGER AND X-RAY PHOTOELECTRON SPECTROSCOPY IN THE STUDY OF ADHESION AND FRICTION

by

Kazuhisa Miyoshi

National Aeronautics and Space Administration  
Lewis Research Center  
Cleveland, Ohio 44135

## Abstract

Three studies are described characterizing the possible contributions of surface science to tribology. These include surface contamination formed by the interaction of a surface with the environment, contaminants obtained with diffusion of compounds, and surface chemical changes resulting from selective thermal evaporation. Surface analytical tools such as Auger electron spectroscopy (AES) and x-ray photoelectron spectroscopy (XPS) incorporated directly into adhesion and friction systems are primarily used to define the nature of tribological surfaces before and after tribological experimentation and to characterize the mechanism of solid-to-solid interaction. Emphasis is on fundamental studies involving the role of surfaces in controlling the adhesion and friction properties of materials emerging as a result of the surface analyses. The materials which have been studied include metals and ceramics such as elemental metals, amorphous alloys (metallic glasses), and silicon-based ceramics.

## INTRODUCTION

Surface analysis and surface science are evolutionary disciplines. A number of surface analysis techniques are now available for studying solid surfaces at the atomic and electronic levels. These techniques include a variety of electronic, photonic, and ionic spectroscopies. Their number is still growing, and one of the most exciting recent developments is that of the scanning tunnelling microscopy. These techniques provide different pieces of information, and, in due course, it should be possible to coordinate them and provide a coherent self-consistent description of the surface (1 to 3).

The development of surface analytical methods has allowed considerable progress in understanding the effects, phenomena, and reactions in tribology in recent years (1 and 2). The techniques used most are AES and XPS (ESCA). Each of these has the ability to determine the composition of the outermost atomic layers of a clean surface or surfaces covered with adsorbed films of gases, lubricants, and frictionally transferred films and provide a description of the surface (4 to 25).

AES and XPS are generally described as "surface analysis" techniques, but this term can be

misleading. Although these techniques derive their usefulness from their intrinsic surface sensitivity, they can also be used to determine the composition of much deeper layers. Such a determination is normally achieved by the controlled erosion of the surface by ion bombardment. AES or XPS analyze the residual surface left after a certain sputtering time. In this way, composition-depth profiles can be obtained which provide a powerful means of analysis for thin films, surface coatings, and their interfaces. Clearly, this capability also makes AES and XPS ideal for studying wear resistant coatings and solid lubricant films (26 to 28). There are, however, a number of practical differences (e.g., detection speed, background and spatial resolution) which generally are more advantageous in Auger profiling.

This paper discusses the ways in which AES and XPS can be usefully applied to fundamental tribology, particularly adhesion and friction. The emphasis is to relate adhesion and friction to reactions at the interface and to the composition of the interface. The subjects to be addressed include (1) surface contamination by the interaction of a surface with the environment, (2) contamination by diffusion, and (3) chemical changes with selective thermal evaporation. Three examples obtained from adhesion and friction experiments will be presented. The surface analytical tools are incorporated directly into the adhesion and friction systems for in situ analysis. The materials to be examined include metals, alloys, and silicon-based ceramics.

Surface studies, such as these, can provide us with a basic understanding of some of the important processes involved in adhesion, friction, lubrication, and wear. In the long run, they may provide us with information that will allow us to select the materials and surface treatments best suited for a particular application (3).

## EXPERIMENTAL

Figure 1 shows a typical apparatus chamber for conducting a surface chemical analysis. The particular system depicted in Figure 1 is used for adhesion and friction studies when two surfaces are in solid-to-solid contact. Details of the mechanisms for measuring adhesion and friction are described elsewhere (29 and 30).

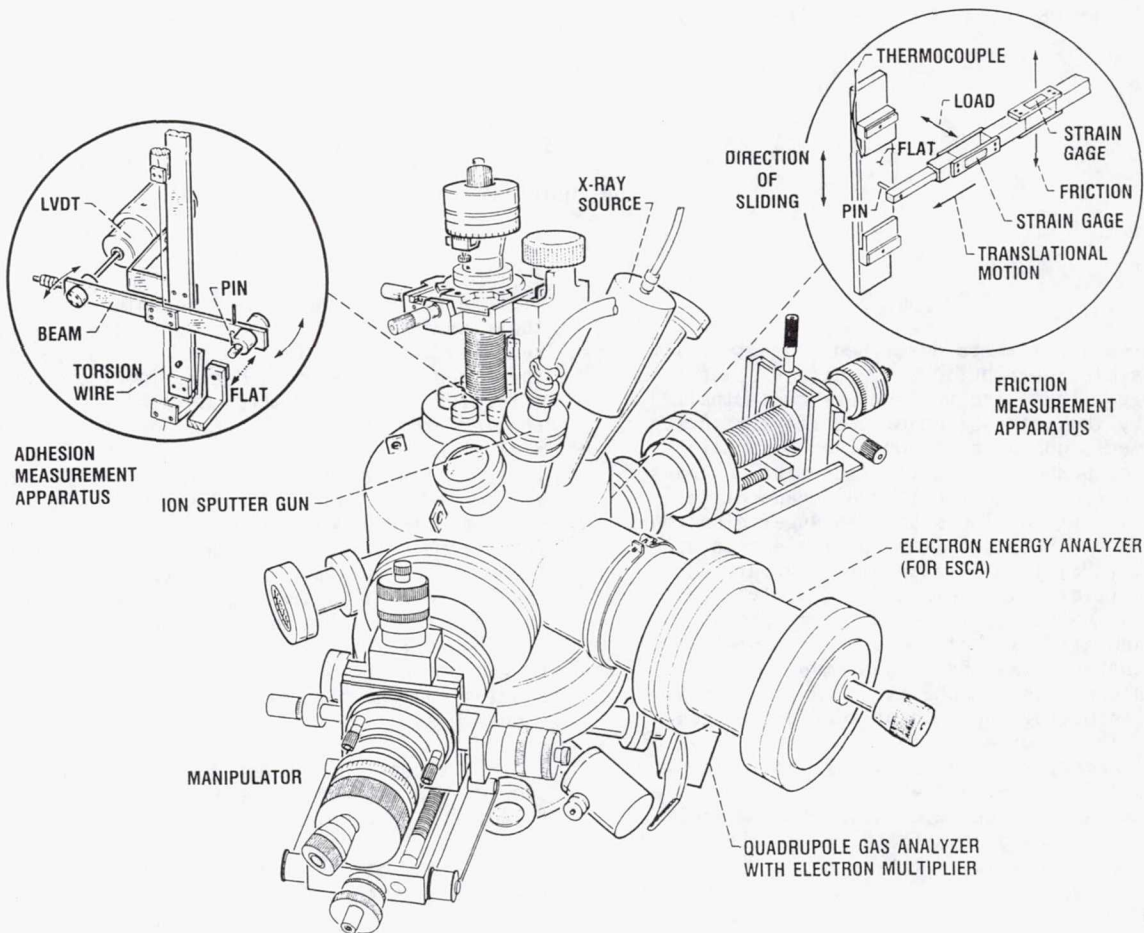


FIG. 1. - APPARATUS FOR MEASURING ADHESION AND FRICTION IN UTRAHIGH VACUUM.

Briefly, the apparatus used in this investigation consisted of an ultrahigh vacuum system capable of measuring adhesion and friction at various temperatures; the vacuum system contained an electron spectrometer for AES and XPS (e.g., Fig. 1). The mechanism for measuring adhesion and friction was basically a pin-on-flat configuration, as shown schematically in Figure 1.

For pulloff force (adhesion) measurements in vacuum, the flat specimen was brought into contact with the pin specimen. Contact was maintained for 30 sec before the pin and flat specimen surfaces were pulled apart. The adhesion measuring device used was a torsion balance adapted from the principle of the Cavendish balance used to measure gravitational forces. Forces as low as 1  $\mu$ N can be measured.

For single-pass sliding friction measurements, the flat specimen was brought into contact with the pin specimen. Contact was maintained for 30 sec before sliding was initiated at a sliding velocity of 3 mm/min. Strain gauges mounted on a manipulator-mounted beam were used to measure loads and forces.

## RESULTS

### Adhesion and Friction of Clean and Contaminated Surfaces

Carbon is ubiquitous: even a supposedly "clean" specimen surface will show a significant carbon contribution to the AES and XPS spectrum because of the presence of one or more layers of adsorbed hydrocarbons and oxides of carbon. Contamination is often an important factor in determining the adhesion and friction properties of surfaces. Contaminant films may form either by the interaction of a surface with the environment or by the diffusion of bulk contaminants through the solid itself.

### Surface Contamination by the Environment

A contamination layer will attenuate the electron signal from the underlying surface, and important features in the spectrum may be masked in this way. XPS survey spectra of the as-received silicon nitride surface reveal an adsorbed carbon peak as well as an oxygen peak, as shown by curve (a) in Figure 2. A layer of

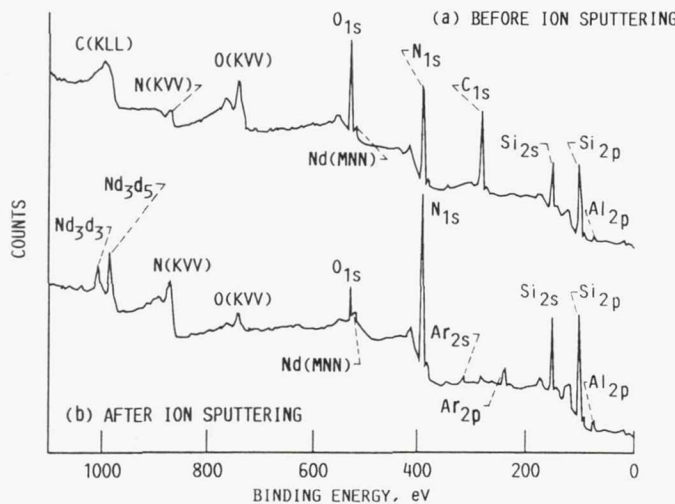


FIG. 2. - X-RAY PHOTOELECTRON SPECTROSCOPY (XPS) SPECTRA OF SILICON NITRIDE OBTAINED BEFORE AND AFTER ION SPUTTERING.

adsorbate on the surface consisted of hydrocarbons and water vapor from the environment that may have condensed and become physically adsorbed to the silicon nitride surface. The contamination layer may be removed by ion etching just prior to or during analysis; but, since the ion beam itself can induce compositional changes in the specimen surface, it must be used with care. After the silicon nitride surface was cleaned by argon ion sputtering, the carbon and oxygen contamination peaks became very small (curve (b) in Fig. 2); the peak intensity of both the silicon and nitrogen associated with silicon nitride increased markedly. The small amount of carbon and oxygen is associated with bulk contaminants of the silicon nitride.

Removing contaminant films from the surfaces of ceramics and metals results in a very strong interfacial adhesion when two such solids are brought into contact. If an atomically clean silicon carbide surface is brought into contact with a clean aluminum surface, the adhesive bonds formed at the silicon carbide - aluminum interface are sufficiently strong so that the cohesive bonds in the aluminum are fractured and, as a result, the aluminum transferred to the silicon carbide surface (31).

Typical pulloff force (adhesion) results from hot-pressed polycrystalline silicon nitride in contact with metals are presented in Figure 3. The marked difference in adhesion for the two surface conditions, the contaminated (as-received) surfaces and sputter-cleaned surfaces, is shown in Figure 3. Contaminant films on the as-received surfaces reduces the adhesion.

The results in ultrahigh vacuum are to be anticipated from chemical interactions and the important role they play in the adhesion of silicon nitride - metal couples. With the contaminated surfaces, however, the chemical activity

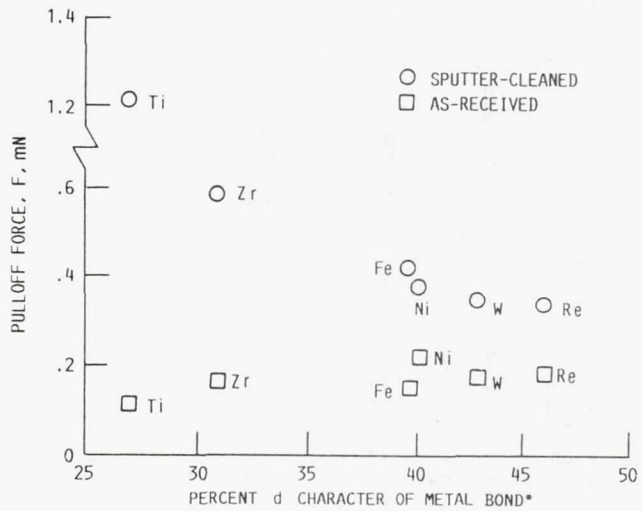


FIG. 3. - PULLOFF FORCE (ADHESION) AS FUNCTION OF PERCENTAGE OF d-BOND CHARACTER OF TRANSITION METALS IN CONTACT WITH MONOLITHIC SILICON NITRIDE IN VACUUM. (\*L. PAULING, "A RESONATING-VALENCE-BOND-THEORY OF METALS AND INTERMETALLIC "COMPOUNDS", PROC. R. SOC. LONDON, SER. A., 196, PP. 343-362 (1949).)

or inactivity of a metal does not appear to play a role in adhesion (Fig. 3). The adhesion for various metals in contact with silicon nitride generally remains constant. A prerequisite for this sameness in adhesion is that the surfaces are covered with a stable layer of contaminants. Thus, contaminant films on the surface of ceramics and metals can greatly reduce adhesion.

In contrast, adhesion is higher for sputter-cleaned surfaces than it is for the as-received surfaces, and adhesion properties are related to the relative chemical activity (percentage d-bond character) of the transition metals as a group. According to Pauling's theory, the greater the percentage of d-bond character, the less active the metal is and the lower the pulloff force is that is required to break the bonds (Fig. 3). Thus, adhesion results (Fig. 3) show that the more active the metal, the higher the adhesion. This is consistent with the earlier friction studies conducted with the surfaces of other nonmetals.

As a result of sliding friction experiments conducted with various transition metals in contact with nonmetallic hard materials such as diamond, silicon carbide, ferrites, and boron nitride coating, it was found that the coefficient of friction is related to the relative chemical activity (d valence bond character) of those metals in ultrahigh vacuum. The more active the metal, the higher the coefficient of friction. Therefore, the coefficient of friction for metals is related to adhesion. The higher the adhesion, the greater the coefficient of friction.

## Surface Contamination by Diffusion

There is another aspect of surface contaminant films which may form by diffusion of bulk contaminants through the solid itself. An example of this type of surface contamination and usefulness of XPS for analysis of surface chemical composition will be demonstrated with the data on three ferrous-based amorphous alloys (metallic glasses).

Single-pass sliding friction experiments were conducted with sputter-cleaned aluminum oxide (sapphire) in contact with sputter-cleaned amorphous alloys in vacuum at temperatures up to 750 °C. The coefficients of friction as a function of temperature of the amorphous alloy specimen are indicated in Figure 4.

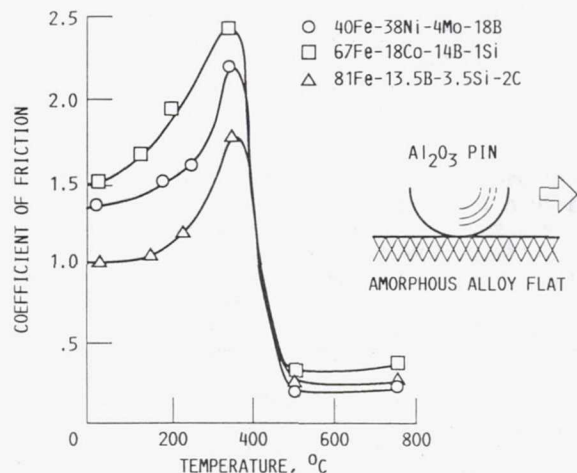


FIG. 4. - COEFFICIENT OF FRICTION AS FUNCTION OF TEMPERATURE FOR ALUMINUM OXIDE PINS SLIDING ON FERROUS-BASED AMORPHOUS ALLOYS (METALLIC GLASSES).

As the temperature increases from room temperature to 350 °C, the friction increases (see Fig. 4). The increase in friction is associated with changes in the thermal, chemical, and microstructural states (32). These alloys then completely transform from the amorphous to the crystalline state between 410 and 480 °C (32).

At 500 °C (in Fig. 4) the friction undergoes a marked decrease from that measured at 350 °C. Why does this appreciable decrease occur? Surface analysis with XPS supplies the answer.

Figure 5 presents the XPS spectra for one of the ferrous-based amorphous alloys of Figure 4 in the as-received condition, after sputter cleaning, when heated to 350 and 750 °C. The XPS spectra of Fe<sub>2p</sub>, Co<sub>2p</sub>, B<sub>1s</sub>, and Si<sub>2p</sub> peaks as function of binding energy are presented.

All the XPS spectra taken from the surfaces of the three amorphous alloys as-received clearly reveal adsorbed carbon and oxygen contaminants in addition to the various alloying constituents of the nominal bulk composition. Beneath this layer of adsorbate is a mixture layer of oxides of the alloying constituents (see Fig. 5).

Sputter cleaning removes the oxides and other contaminants from the alloy surface. The argon-sputter-cleaned surface consisted of the alloy and small amounts of oxides and carbides (32).

In addition to nominal element constituents, the surface that is argon sputter cleaned and then heated to 350 °C contains boric and silicon oxides on 67Fe-18Co-14B-1Si (Fig. 5) and 81Fe-13.5B-3.5Si-2C alloys and boric oxides on 40Fe-38Ni-4Mo-18B alloys as well as small amounts of carbides that migrated from the bulk of the alloys by heating.

The surface that is argon sputter cleaned and then heated to 500 and 750 °C contains boron nitride that migrated from the bulk of the alloys as well as small amounts of oxides. The cause for the marked reduction in friction at 500 and 750 °C in Figure 4 is related to the presence of boron nitride on the surface of the alloy, as typically indicated at 750 °C in Figure 5(c). Boron nitride is also present at 500 °C. Boron nitride is a solid lubricant and brings about the friction reduction observed in Figure 4. Thus, examinations of the surface chemistry in the heating stage give valuable information on the behavior of surface contamination caused by diffusion. The diffusion of contaminants such as boron nitride or oxides are responsible for the friction behavior.

## Chemical Changes with Selective Thermal Evaporation

In general, AES provides elemental information (i.e., an elemental analysis) only. The Auger peaks of many elements, however, show significant changes in position or shape in different chemical environments (1). For example, it is possible to distinguish among amorphous carbon, carbide-type carbon, and graphitic carbon in AES (Fig. 6). On the other hand, the main advantage of XPS is its ability to provide chemical information from the shifts in binding energy, as also shown in Figure 7. Thus, Figures 6 and 7 present a comparison of the AES and XPS carbon peaks for carbon in various forms present on the single-crystal silicon carbide. The AES and XPS spectra of the single-crystal silicon carbide were obtained from the as-received surface and the surface heated to 800 and 1500 °C.

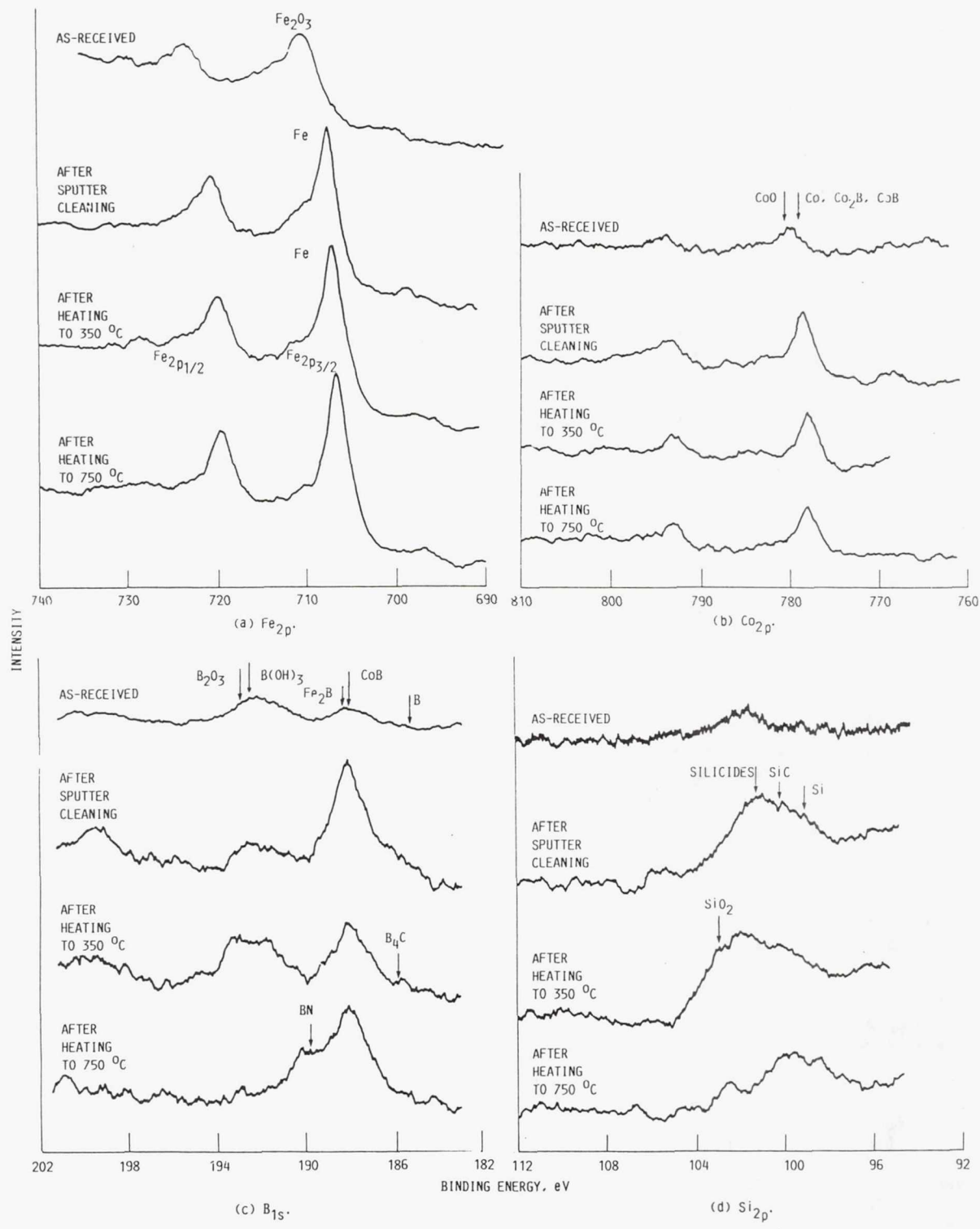


FIG. 5. - REPRESENTATIVE  $\text{Fe}_{2p}$ ,  $\text{Co}_{2p}$ ,  $\text{B}_{1s}$ , AND  $\text{Si}_{2p}$  XPS PEAKS ON 67Fe-18Co-14B-1Si.

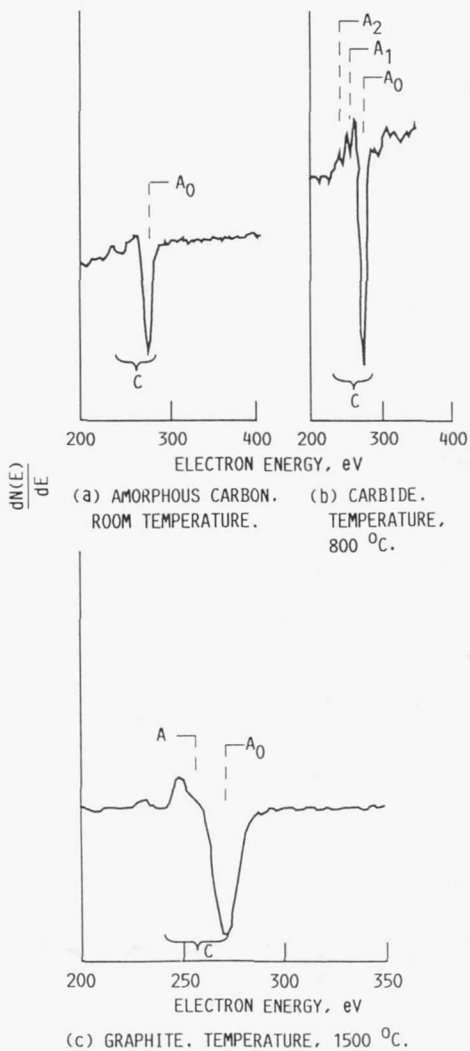


FIG. 6. - AUGER PEAKS OF CARBON ON SILICON CARBIDE (0001) SURFACE.

Figure 6 shows the typical AES amorphous carbon-type, carbide-type, and graphite-type carbon peaks. When an as-received silicon carbide is placed in a vacuum, one of the principal contaminants on the as-received silicon carbide surface is adsorbed carbon. The AES peak for carbon appears only as the single main carbon peak labeled  $A_0$  in Figure 6(a), where  $A$  is used to denote an AES peak. The AES peak is similar to that obtained for amorphous carbon but not carbide (31). The AES peaks for carbon on the surface heated to 800 °C indicate a carbide-type carbon peak, similar to that obtained for an argon-sputter-cleaned surface. The carbide-type peaks are characterized by the three peaks labeled  $A_0$ ,  $A_1$ , and  $A_2$  in Figure 6(b). The spectra of the surface heated above 800 °C clearly reveal a graphite-type carbon peak at 271 eV, as typically indicated at 1500 °C (see Fig. 6(c)). The graphite form is characterized by a step (labeled  $A$  in Fig. 6(c)).

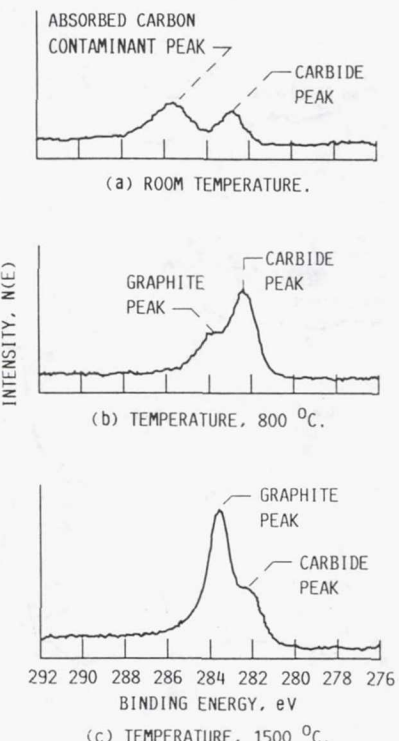


FIG. 7. - XPS PEAKS OF CARBON ON SILICON CARBIDE (0001) SURFACE.

In XPS spectra photoelectron lines for  $C_{1s}$  of the silicon carbide are split asymmetrically into doublet peaks, as shown in Figure 7. Three spectral features, which are dependent on the chemical nature of the specimen, are observed: (1) two kinds of doublet peaks, (2) change of the vertical height of the peaks, and (3) shift of peaks. The XPS spectra of the as-received surface indicate distinguishable kinds of carbon - that is, a carbon contamination peak and a carbide peak associated with the silicon carbide. The peak height of the carbon contamination is higher than that of the carbide. For specimen heated to 800 °C, a large carbide and a small graphite peak are seen in the spectra. The spectra of the surface heated above 800 °C indicate a very large graphite peak and a small carbide peak, as typically seen at 1500 °C (Fig. 7(c)). Thus, the physical conclusion from the AES and XPS surface analyses is that temperature affects the surface chemistry significantly and the surface of silicon carbide graphitizes.

It is interesting to note that the AES analysis of silicon carbide heated to 1500 °C indicated that the carbon peak shown was only of the graphite form (Fig. 6(c)). The XPS analysis, however, indicated carbide as well as graphite was present on the silicon carbide surface heated to 1500 °C (Fig. 7(c)). This difference can be accounted for by the fact that the analysis depth with XPS is deeper. Table I presents the estimated thickness of the graphite layer formed on

TABLE I. - VALUES FOR THE THICKNESS OF THE GRAPHITE LAYER ON THE SILICON CARBIDE SURFACE PREHEATED TO 1500 °C

Element and photoelectron, Mg $\text{K}\alpha$	Electron inelastic mean free path, $\lambda$ , nm	Thickness of layer, $d$ , nm
Si <sub>2p</sub>	a <sub>4.7</sub>	2.0
	a <sub>3.9</sub>	1.7
C <sub>1s</sub>	b <sub>4.4</sub>	1.8
Graphite C <sub>1s</sub>	a <sub>2.1</sub>	1.5
	a <sub>3.1</sub>	2.3
	a <sub>3.4</sub>	2.4

<sup>a</sup>Evans, S., Pritchard, R.G., and Thomas, J.M., "Escape Depths of X-ray (Mg-K-Alpha)-induced Photoelectrons and Relative Photoionization Cross-Sections for the 3p Subshell of the Elements of the First Long Period," *J. Phys. C.*, 10, 13, pp. 2483-2498 (July 1977).

<sup>b</sup>Cadman, P., Evans, S., Scott, J.D., and Thomas, J.M., "Determination of Relative Electron Inelastic Mean Free Paths (Escape Depths) and Photoionization Cross-Sections by X-ray Photoelectron Spectroscopy," *J. Chem. Soc., Faraday Trans. II*, 71, 10, pp. 1777-1784 (1975).

the silicon carbide surface (33). The thickness of the outermost surficial graphite layer on the silicon carbide heated to 1500 °C is 1.5 to 2.4 nm. This result suggests that the collapse of the carbon of two or three successive silicon carbide surficial layers after evaporation of the silicon is the most probable mechanism for the graphitization of the silicon carbide surface.

An increase in the surface temperature of a ceramic material or metal tends to promote surface chemical reactions and to volatilize some element. These chemical reactions cause products such as graphite to appear on the surface and, thus, can alter adhesion and friction. Figures 8 and 9 present the average pulloff forces (adhesion) and the coefficient of friction for the as-received silicon carbide (0001) surfaces in contact with a sputter-cleaned polycrystalline silicon carbide pin as a function of temperature in a vacuum. The adhesion characteristics are the same as those for friction. The adhesion and friction generally remain low at temperatures to 300 °C. The low adhesion and friction can be associated with the presence of the carbon contaminants on the as-received flat specimen surface.

Adhesion and friction increase rapidly between 300 and 400 °C. Although adhesion and friction decrease slightly at 600 °C, they remain relatively high between 400 and 700 °C. The rapid increase in adhesion and friction between 300 and 400 °C can be attributed to the absence of adsorbed contaminants such as carbon.

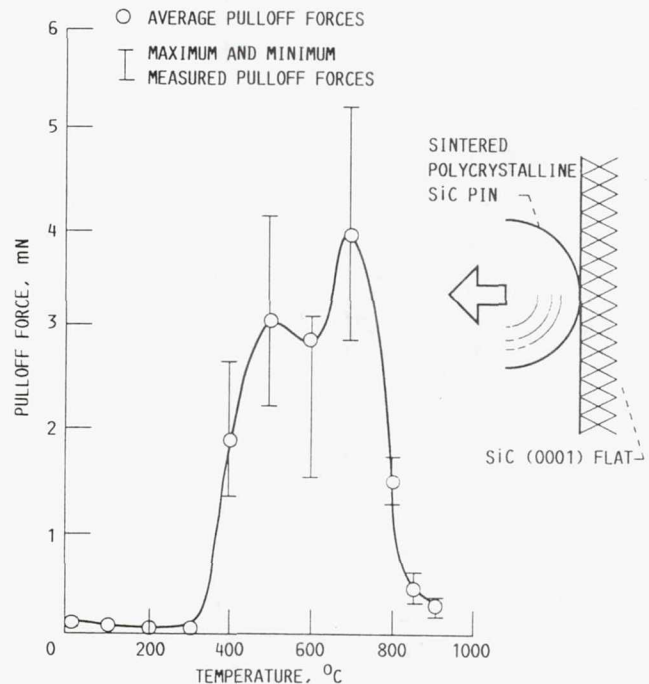


FIG. 8. - PULLOFF FORCE (ADHESION) AS FUNCTION OF TEMPERATURE FOR SILICON CARBIDE (0001) FLAT SURFACES IN CONTACT WITH SINTERED POLYCRYSTALLINE SILICON CARBIDE PINS IN VACUUM.

The somewhat low values of adhesion and friction at 600 °C are probably due to the  $\alpha\text{-SiO}_2$  to  $\beta\text{-SiO}_2$  transition of a small amount of silicon dioxide at about 583 °C and changes in the amount of silicon dioxide on the single-crystal silicon carbide surface and on the sintered polycrystalline silicon carbide surface (34 and 35). Figure 10 presents the XPS peak heights of Si<sub>2p</sub> and O<sub>1s</sub>. These peaks are associated with silicon dioxide on a single-crystal silicon carbide surface and on a sintered polycrystalline silicon carbide surface as a function of a heating temperature. The peak heights of Si<sub>2p</sub> and O<sub>1s</sub> (Si<sub>2p</sub> and O<sub>1s</sub> associated with silicon dioxide) remained high at temperatures to 600 °C. The amount of silicon dioxide on the silicon carbide surfaces increased slightly around 600 °C. The somewhat low values of adhesion and friction at 600 °C are related to the slight increase in the amount of silicon dioxide.

Above 600 °C the peak heights of Si<sub>2p</sub> and O<sub>1s</sub> (Si<sub>2p</sub> and O<sub>1s</sub> associated with silicon dioxide) obtained from the silicon carbide surfaces decrease rapidly with increasing temperature (Fig. 10). This rapid decrease in the amount of silicon dioxide correlates with the increase in adhesion and friction.

Above 800 °C, the adhesion and friction decrease rapidly with an increase in temperature. This rapid decrease in adhesion and friction

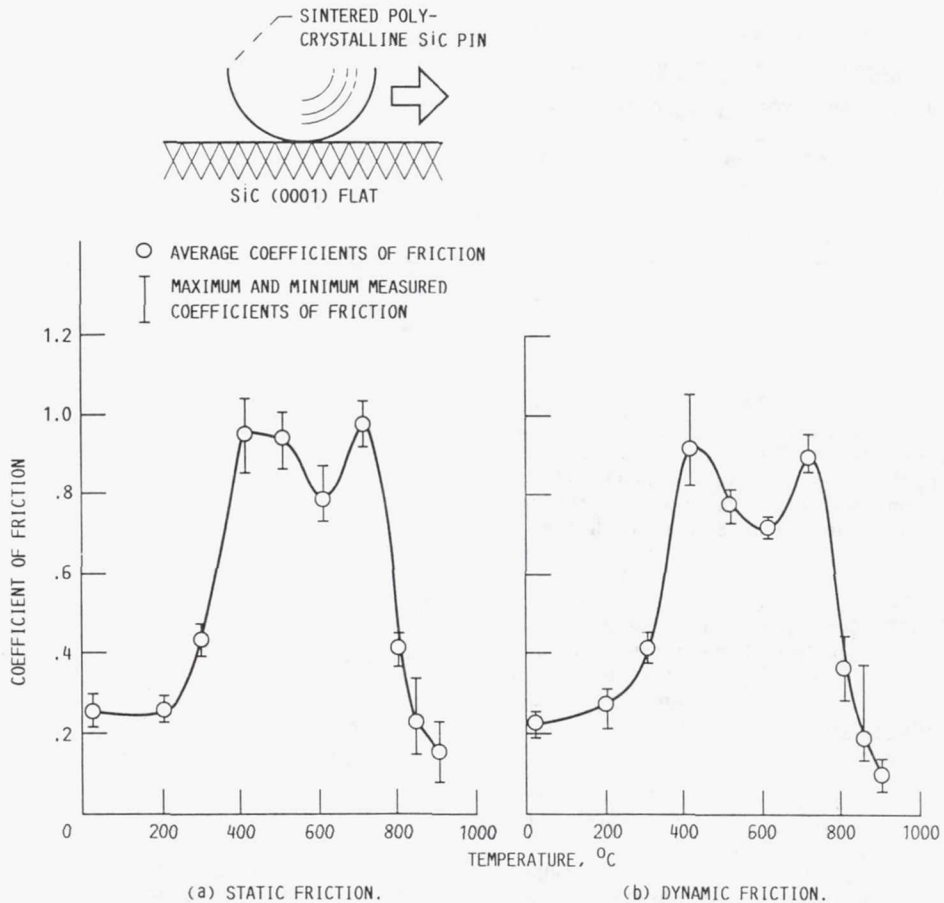


FIG. 9. - COEFFICIENTS OF STATIC AND DYNAMIC FRICTION AS FUNCTIONS OF TEMPERATURE FOR SILICON CARBIDE (0001) FLAT SURFACES IN CONTACT WITH SINTERED POLYCRYSTALLINE SILICON CARBIDE PINS IN VACUUM.

above 800 °C correlates with the graphitization of the silicon carbide surface. Thus, the use of AES and XPS to study the silicon carbide surface reveals that the reduction of adhesion and friction at 800 °C in Figures 8 and 9 is the result of the graphitization of the silicon carbide surface which occurs with heating. The AES and XPS analyses complimented each other in this determination. These experimental results reveal the value of surface analytical tools in the characterization of tribological surfaces.

#### CONCLUDING REMARKS

Three simple examples are given from the *in situ* adhesion and friction experiments in which XPS and AES surface analyses have contributed significantly to the elucidation of phenomena, reactions, and processes in tribology.

1. Surface contaminant films formed by the interaction of a surface with the environment affect the adhesion and friction behavior of surfaces. An adsorbed carbon contaminant on a silicon nitride surface can greatly reduce the adhesion and, accordingly, friction. When clean

ceramics are in contact with clean metals, chemical activity or inactivity is extremely important to adhesion and friction behavior. With the transition metals the d valence bond character correlates directly with the adhesion and the coefficient of friction for ceramics. The higher the percent d-bond character, the lower the adhesion and friction.

2. Contaminants can diffuse from the bulk of ferrous-based amorphous alloys (metallic glasses) to the surface upon heating. Compounds such as boric oxide and/or silicon oxide form on the surface at 350 °C; above 500 °C, boron nitride forms on the surface. The formation and segregation of these contaminants are responsible for the adhesion and friction behavior.

3. Heating silicon carbide to a high temperature can result in selective thermal evaporation. Silicon volatilizes and leaves behind a graphitic surface with the graphitic film functioning to reduce adhesion and friction.

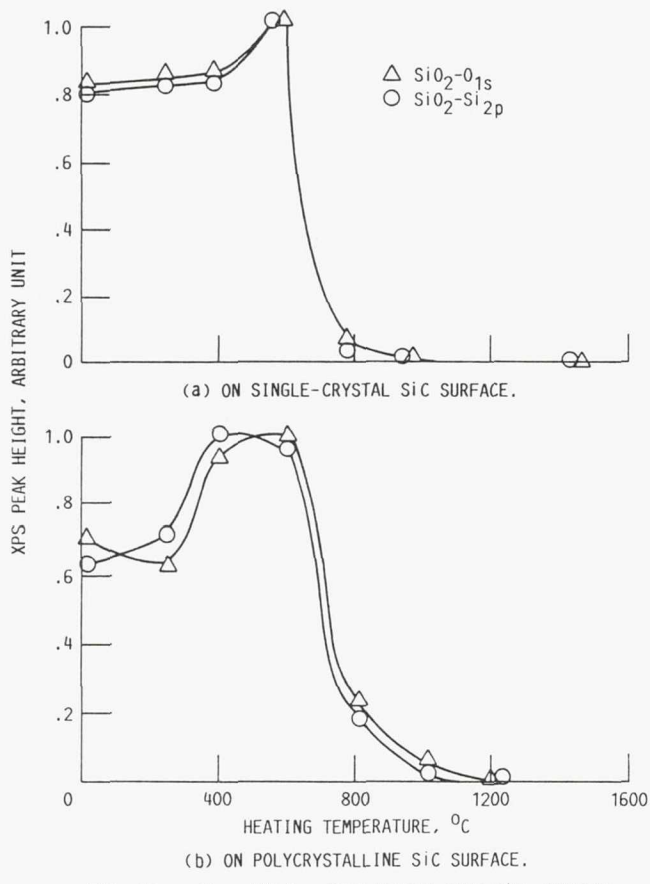


FIG. 10. -  $\text{Si}_{2p}$  AND  $\text{O}_{1s}$  PEAK HEIGHT FROM  $\text{SiO}_2$  PRESENT.

#### REFERENCES

1. Buckley, D.H., "Surface Effects in Adhesion, Friction, Wear and Lubrication," *Tribology Series*, Vol. 5, Elsevier (1981).
2. Buckley, D.H., "The Use of Analytical Surface Tools in the Fundamental Study of Wear," *Wear*, 46, pp. 19-53 (1978).
3. Tabor, D., "Status and Direction of Tribology as a Science in the 80's - Understanding and Prediction," *New Directions in Lubrication, Materials, Wear and Surface Interactions: Tribology in the 80's*, Loomis, W.R., ed., Noyes Publications, Park Ridge, NJ, pp. 1-17 (1985).
4. Woodruff, D.P. and Delchar, T.A., *Modern Techniques of Surface Science*, Cambridge Solid State Science Series, Cambridge University Press (1986).
5. Hantsche, H., "Comparison of Basic Principles of the Surface-Specific Analytical Methods—AES/SAM, ESCA (XPS), SIMS, and ISS with X-Ray Microanalysis, and Some Applications in Research and Industry," *Scanning*, 11, pp. 257-280 (1989).
6. Brewis, D.M., ed., *Surface Analysis and Pretreatment of Plastics and Metals*, Macmillan Publishing Co., Inc. (1982).
7. Briggs, D. and Seah, M.P., *Practical Surface Analysis*, John Wiley & Sons (1983).
8. Pepper, S.V., "Effect of Adsorbed Films on Friction of  $\text{Al}_2\text{O}_3$ -Metal Systems," *J. Appl. Phys.*, 47, pp. 2579-2583 (1976).
9. Pepper, S.V., "Diamond (III) Studied by Electron-Energy Loss Spectroscopy in the Characteristic Loss Region," *J. Vac. Sci. Technol.*, 20, pp. 643-646 (1982).
10. Ferrante, J., "Applications of Surface Analysis and Surface Theory in Tribology," *Surface and Interface Analysis*, 14, pp. 809-822 (1989).
11. Phillips, M.R., Dewey, M., Hall, D.D., Quinn, T.F.J., and Southworth, H.N., "The Application of Auger Electron Spectroscopy to Tribology," *Vacuum*, 26, pp. 451-456 (1976).
12. Baldwin, B.A., "Relationship Between Surface Composition and Wear: X-Ray Photoelectron Spectroscopic Study of Surfaces Treated with Organosulfur Compounds," *ASLE Trans.*, 19, pp. 335-344 (1976).
13. Baldwin, B.A., "Relative Antiwear Efficiency of Boron and Sulfur Surface Species," *Wear*, 45, pp. 345-353 (1977).
14. Bird, R.J. and Galvin, G.D., "The Application of Photoelectron Spectroscopy to the Study of E.P. Films on Lubricated Surfaces," *Wear*, 37, pp. 143-167 (1976).
15. McCarrol, J.J., Mould, R.W., Silver, H.B., and Sims, M.L., "Auger-Electron Spectroscopy of Wear Surfaces," *Nature*, 266, 5602, pp. 518-519 (1977).
16. Shafrin, E.G. and Murday, J.S., "Analytic Approach to Ball-Bearing Surfaces Chemistry," *J. Vac. Sci. Technol.*, 14, pp. 236-253 (1977).
17. Shafrin, E.G. and Murday, J.S., "Auger Compositional Analysis of Ball Bearing Steels Reacted With Tricresyl Phosphate," *ASLE Trans.*, 21, pp. 329-336 (1978).
18. Murday, J.S. and Shafrin, E.G., "Surface Chemistry at Ball Bearing Steel II," Naval Research Lab., NRL-MR-3850 (1978).
19. Singer, I.L. and Murday, J.S., "Investigation of Lubricated Bearing Surfaces by X-Ray Photoelectron and Auger Electron Spectroscopies," *Fundamentals of Tribology*, N.P. Suh and N.A. Saka, eds., MIT Press, Cambridge, MA, pp. 239-252 (1980).
20. Bennett, M.R., Kinzig, B.J., Murday, J.S., and Ravner, H., "Surface Analysis of Bearing Steels After Solvent Treatments," *ASLE Preprint No. 79-LC-4D-2* (1979).
21. Wheeler, D.R., "X-Ray Photoelectron Spectroscopic Study of Surface Chemistry of Dibenzyl Disulfide on Steel Under Mild and Severe Wear Conditions," *Wear*, 47, pp. 243-254 (1978).
22. Wheeler, D.R., "Surface Chemistry of Iron Sliding in Air and Nitrogen Lubricated with Hexadecane and Hexadecane Containing Dibenzyl-Disulfide," *NASA TP-1545* (1979).

23. Debies, T.P., and Johnston, W.G., "Surface Chemistry of Some Antiwear Additives as Determined by Electron Spectroscopy," ASLE Trans., 23, 3, pp. 289-297 (1980).

24. Brainard, W.A., and Ferrante, J., "Evaluation and Auger Analysis of a Zinc-Dialkyl-Dithiophosphate Antiwear Additive in Several Diester Lubricants," NASA TP-1544 (1979).

25. Oppelt, J., Mueller, K., and Bartz, W.J., "Wear Scar Analysis by Ion Beam Technology," ASLE Preprint No. 79-LC-2B-4 (1979).

26. Wheeler, D.R., "Application of ESCA to the Determination of Stoichiometry in Sputtered Coatings and Interface Regions," NASA TM-78896 (1978).

27. Miyoshi, K., "Fundamental Tribological Properties of Ion-Beam-Deposited Boron Nitride Thin Films," Mater. Sci. Forum, 54-55, pp. 375-398 (1990).

28. Miyoshi, K., Pouch, J.J., and Alterovitz, S.A., "Plasma-Deposited Amorphous Hydrogenated Carbon Films and Their Tribological Properties," Mater. Sci. Forum, 52-53, pp. 645-656 (1989).

29. Miyoshi, K., Pouch, J.J., Alterovitz, S.A., Pantic, D.M., and Johnson, G.A., "Adhesion, Friction, and Wear of Plasma-Deposited Thin Silicone-Nitride Films at Temperatures to 700 °C," Wear, 133, pp. 107-123 (1989).

30. Miyoshi, K., Maeda, C., and Masuo, R., "Development of a Torsion Balance for Adhesion Measurements," IMEKO XI: Instrumentation for the 21st Century; Proceedings of the 11th Triennial World Congress of the International Measurement Confederation (IMEKO), Houston, TX, 16-21 Oct. 1988, Instrument Society of America, Research Triangle Park, N.C., pp. 263-278, (1988).

31. Miyoshi, K., and Buckley, D.H., "Considerations in Friction and Wear," New Directions in Lubrication, Materials, Wear and Surface Interactions. Tribology in the 80's, W.R. Loomis, ed., Noyes Publications, Park Ridge, NJ, pp. 282-319 (1985).

32. Miyoshi, K., and Buckley, D.H., "Microstructure and Surface-Chemistry of Amorphous-Alloys Important to Their Friction and Wear Behavior," Wear, 110, pp. 295-313 (1986).

33. Miyoshi, K., and Buckley, D.H., "Surface Chemistry and Wear Behavior of Single-Crystal Silicon Carbide Sliding Against Iron at Temperatures to 1500 °C in Vacuum," NASA TP-1947 (1982).

34. Weast, R.C., ed., CRC Handbook of Chemistry and Physics, 68th ed., CRC Press Inc., Boca Raton, FL (1987).

35. Miyoshi, K., Buckley, D.H., and Srinivasan, M., "Tribological Properties of Sintered Polycrystalline and Single-Crystal Silicon Carbide," American Ceramic Society Bulletin, 62, 4, pp. 494-500 (1983).



National Aeronautics and  
Space Administration

## Report Documentation Page

1. Report No. NASA TM-103266	2. Government Accession No.	3. Recipient's Catalog No.	
4. Title and Subtitle Uses of Auger and X-ray Photoelectron Spectroscopy in the Study of Adhesion and Friction		5. Report Date	
		6. Performing Organization Code	
7. Author(s) Kazuhisa Miyoshi	8. Performing Organization Report No. E-5631	10. Work Unit No. 506-43-11	
9. Performing Organization Name and Address National Aeronautics and Space Administration Lewis Research Center Cleveland, Ohio 44135-3191	11. Contract or Grant No.	13. Type of Report and Period Covered Technical Memorandum	
12. Sponsoring Agency Name and Address National Aeronautics and Space Administration Washington, D.C. 20546-0001	14. Sponsoring Agency Code		
15. Supplementary Notes Prepared for the First International Symposium on Industrial Tribology sponsored by the National Science Foundation Industry/University Cooperative Research Center for Engineering Tribology at Northwestern University, Illinois, August 29-31, 1990.			
16. Abstract Three studies are described characterizing the possible contributions of surface science to tribology. These include surface contamination formed by the interaction of a surface with the environment, contaminants obtained with diffusion of compounds, and surface chemical changes resulting from selective thermal evaporation. Surface analytical tools such as Auger electron spectroscopy (AES) and x-ray photoelectron spectroscopy (XPS) incorporated directly into adhesion and friction systems are primarily used to define the nature of tribological surfaces before and after tribological experimentation and to characterize the mechanism of solid-to-solid interaction. Emphasis is on fundamental studies involving the role of surfaces in controlling the adhesion and friction properties of materials emerging as a result of the surface analyses. The materials which have been studied include metals and ceramics such as elemental metals, amorphous alloys (metallic glasses), and silicon-based ceramics.			
17. Key Words (Suggested by Author(s)) AES XPS Adhesion Friction	18. Distribution Statement Unclassified - Unlimited Subject Category 27		
19. Security Classif. (of this report) Unclassified	20. Security Classif. (of this page) Unclassified	21. No. of pages 11	22. Price* A03